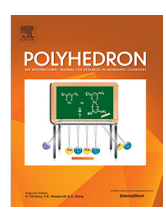
ELSEVIER

Contents lists available at ScienceDirect

Polyhedron

journal homepage: www.elsevier.com/locate/poly



Carbon as an electron donor atom

Steve Scheiner 1

Department of Chemistry and Biochemistry, Utah State University, Logan, UT 84322-0300, United States



ARTICLE INFO

Article history: Received 23 September 2020 Accepted 30 October 2020 Available online 9 November 2020

Keywords:
Tetrel bond
Pnicogen bond
Chalcogen bond
Halogen bond
Carbene
Ditetrel bond

ABSTRACT

There are a number of C-containing entities which can donate electrons. The C atom of the CN $^-$ anion contains a lone pair which can be transferred to a Lewis acid. Even if the acid molecule is anionic, short-range attractive forces can overcome the long-range ion-ion repulsion to approach close enough to engage in a strong bonding interaction. The CN $^-$ anion can be surrounded by a number of ligands that interact through a host of different types of bonds. The C lone pair of the MeCH $_2^-$ carbanion is also available for donation. Neutral C-containing molecules can function as electron source as well. Despite the absence of any C lone pair, a CH $_3$ M unit can donate electron density from its σ -bonding orbitals to a neutral molecule within the framework of a ditetrel bond. The C lone pairs of carbenes may also be donated to form strong bonds within the covalent range. The π -systems of alkenic or aromatic molecules represent an alternate source, although generally weaker than the interactions arising from C lone pairs.

© 2020 Elsevier Ltd. All rights reserved.

1. Introduction

In the classic description of the AH \cdots B H-bond (HB), there is a lone electron pair on the base B which is partially donated to the acid AH [1–4]. More specifically, the lone pair density is shifted primarily into the $\sigma^*(AH)$ antibonding orbital. It is this transfer which is responsible for the weakened AH covalent bond, manifested by its elongation and the red shift of its stretching frequency. This charge donation is of course only part of the story, as there are also strong elements of Coulombic attraction between the two subunits, internal polarization, and dispersion forces. But the transfer component contains elements of a dative bond, involving the formation of a partial covalent bond between the two subunits.

It is not only the HB for which these sorts of phenomena contribute to a strong interaction. The replacement of the bridging H by any of a wide range of electronegative elements presents a very similar situation in nearly all particulars. The halogen bond (XB) offers one of several examples [5–14]. The partial overall negative charge on the X atom of RX is offset by a positive region lying directly along the extension of the R-X covalent bond. This so-called σ -hole provides the same welcome to the negative region of the base as does the bridging H in a HB. The situation is very similar when X is replaced by elements of various other families of the periodic table, leading as well to chalcogen, pnicogen, and tetrel bonds [15–27]. In all these cases, the stability of the bond arises in part from the partial donation of the lone pair of the

approaching base to the Lewis acid, fitting the description of a partial covalent dative bond.

The vast majority of prior work on these sorts of bonds has concerned itself with the standard bases characterized by lone pairs on O, N, or F atoms which directly engage with the Lewis acid. But there are also alternative situations where the electrons may come from C atoms on the base as well. It is this sort of situation which represents the focus of this article. There are a number of specific sources of this type. One major example is the C lone electron pair on the CN⁻ anion. The full charge of this species adds to its ability to interact with an acid, while also presenting a hindrance as is discussed below. A standard RCH₂ carbanion, where R refers to any alkyl group, also offers a C lone pair for possible dative bond formation, as do any of several neutral carbenes. The exploration extends further to other sorts of C electron donors, even those without lone pairs. The electrons may come, for example, from the π -system of alkene systems, conjugated or otherwise, as well as aromatic units. Another option would extract electrons from σ -bonding orbitals, as is detailed below.

1.1. CN⁻ as prototypical electron pair donor

The CN⁻ anion is a small but interesting species. Its small size imbues it with a high charge density, making it a potent nucle-ophile. The classical Lewis structure places a lone pair on both the C and N atoms, either of which could engage in a dative bond with an electron-poor species. More detailed examination of the molecular electrostatic potential that surrounds CN⁻ would categorize it as roughly isotropic. This MEP contains minima on both

¹ ORCID: 0000-0003-0793-0369. *E-mail address:* steve.scheiner@usu.edu

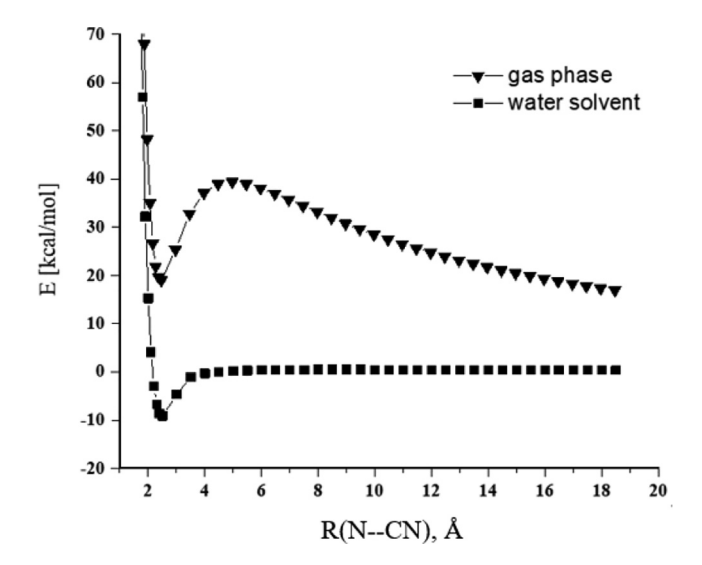


Fig. 1. Dissociation potential of $X_nM^-\cdots CN^-$ complex at the MP2/aug-cc-pVDZ level. Zero of energy is taken as that of the fully dissociated monomers for both gas phase and aqueous solvent.

ends along the C—N axis [28] that are very nearly identical in value. There is also a belt of minimum MEP around the equator of this molecule. So at least on a purely electrostatic basis, an electrophile could attack almost any place around this anion. This anion has thus been employed in a number of situations where it can attack an electrophile.

1.1.1. Interactions with other anions

A first set of examples demonstrate the power of this species by pairing it with another anion. MCl_3^- where M represents one of the alkaline earth metals Be, Mg, Ca, Sr, or Ba [28] pairs with CN^- in a stable complex, despite its negative charge which one would expect to strongly repel CN^- . MCl_3^- is of D_{3h} symmetry, in a trigonal planar structure, and the CN^- attacks the M atom from above the plane. There is an energetic preference for the N atom for the four heavier M atoms, but C is preferred for M = Be. However, this preference for N is a small one in any case, less than 1 kcal/mol, while the C binding preference of Be is a little larger, at 1.6 kcal/mol.

Regardless of the slight preference for C or N end, what is remarkable about the interaction is that it involves a pair of anions. Simple chemical intuition would suggest a purely repulsive interaction, yet quantum calculations [28] yielded a true minimum for their interaction, with an intermolecular distance that varied from 1.8 Å for the smallest Be to 2.9 Å for Ba. AIM analysis of the bond critical point suggested the bond was largely noncovalent with positive values of both ρ and its Laplacian, but the energy density H was negative for the Be-C bond, hinting at some small measure of covalent/dative character.

A central question emerges as to what phenomenon would be responsible for holding a pair of anions together. It must first be understood that this complex is of only metastable character. That is, as the two subunits are pulled apart from their equilibrium geometry, there is an initial rise in energy. But further removal from that point then leads to a progressive stabilization. Indeed, a full dissociation into a pair of isolated CN⁻ and MCl₃⁻ anions is more stable than is the complex. A typical such potential is exhibited in the upper diagram of Fig. 1. The barrier which the complex must climb over to reach the pair of dissociated anions is between 18 and 22 kcal/mol, so is a substantial one. One interpretation of this phenomenon would be that if the two anions can be pulled

in close enough, a dative bond can begin to form between them, pulling them in closer to one another in a metastable complex.

The preceding places the two anions in an in vacuo environment, where the anion-anion repulsion would be at its unfiltered highest. If instead they are situated in a solvent, the surrounding molecules can help to shield each anion from the electrostatic repulsion of the other. Thus the initial mutual repulsion will be less repulsive, and the two can more easily approach to within bonding range. In fact, this is the scenario that is observed [28]. In the context of a model aqueous solvent, as in the lower diagram of Fig. 1, the approach of the two anions from long distance is energetically downhill, with no barrier. The bimolecular complex is fully stable, rather than metastable. And the energetics of the binding are remarkably robust. The interaction energies in aqueous solution vary from a minimum of 1.2 kcal/mol for BaCl₃, all the way up to 33.1 kcal/mol for the smallest M in BeCl₃, which binds directly to the C atom of CN⁻.

These same sorts of idea are not limited to alkaline earth metals of the Group 2A. Substitution of M by the Group 2B metal atoms Zn, Cd, and Hg [29] led to similar findings. One difference is that these M atoms much more strongly prefer the C over the N end of CN⁻, by between 5 and 13 kcal/mol. So all of these complexes might be fit into the category of a C-dative bond between C and M. The R(C-M) distances are between 2.0 and 2.2 Å, which impart to them a certain degree of covalency. This idea is buttressed by negative values of H in the AIM analysis, as well as large bond critical point densities, some surpassing 0.1 au. Like the 2A correlates, the two anions engage in a metastable equilibrium complex in the gas phase, here with dissociation barriers of 24–26 kcal/mol. And again, the situation is quite different in aqueous solution where strong stable complexes are formed, whose dissociation is steadily uphill energetically. These interaction energies in Table 1 are all higher than 15 kcal/mol, with binding energies in the 11-18 kcal/mol range.

Nor are these ideas limited to metal atoms of groups 2A and 2B. The same sort of phenomena occur when it is a pnicogen atom from group 5A that is associating with the CN^- anion [30]. ZCl_4^- anions, with Z = P, As, and Sb, also prefer the C end of the anion. These interactions are even stronger. In the first place, the R ($Z\cdots C$) distances are between 1.8 and 2.2 Å. Secondly, the AIM quantities are even more suggestive of covalent bonding elements, with ρ larger than 0.1 au, and H uniformly negative.

Perhaps more important are the energetics. The interaction energies in Table 1 surpass 50 kcal/mol, at least twice as large as those encountered for the metal atoms in the table. The binding

Table 1 Interaction and binding energies (E_{int}, E_b) of $NC^- \cdots MCl_3^-$ and $NC^- \cdots ZCl_4^-$ complexes calculated at the MP2/aug-cc-pVDZ level in aqueous solution. Also listed are the electrostatic component of the interaction energy (E_{el}) and π -hole depth $(V_{s,max})$. All in kcal/mol.

Complex	E_{int}	E_b	E_{el}	$V_{s,max}$
2A				
NC [−] ···BeCl ₃	-33.07	-19.55	-6.5	-72.1
$CN^- \cdots MgCl_3^-$	-16.94	-15.75	-0.8	-2.0
$CN^- \cdots CaCl_3^-$	-7.96	-7.80	2.1	43.5
$CN^- \cdot \cdot \cdot SrCl_3^-$	-5.50	-5.47	0.1	34.4
$CN^- \cdots BaCl_3^-$	-1.24	-1.24	3.0	28.6
2B				
$NC^- \cdot \cdot \cdot ZnCl_3^-$	-25.80	-18.36	-41.8	-56.4
$NC^- \cdot \cdot \cdot CdCl_3^-$	-16.06	-12.09	-37.3	-44.8
$NC^- \cdot \cdot \cdot HgCl_3^-$	-20.78	-11.43	-97.0	-61.4
5A				
NC⁻···PCl₄	-69.46	-22.56	-111.1	-72.5
NC⁻···AsCl₄	-61.02	-23.06	-99.0	-62.9
$NC^- \cdot \cdot \cdot SbCl_4^-$	-50.50	-22.54	-78.2	-52.1

energies in the next column are also larger than their M counterparts, but the large discrepancy between E_{int} and E_b requires some elaboration. The binding energy is defined as the reaction energy taking a pair of isolated optimized monomers into the complex. The interaction energy takes as its reference the two monomers after they have adjusted their internal geometries to that which they adopt within the complex. So these two quantities differ by the deformation energy required for this monomer adjustment to take place. These deformation energies were reasonably small for the MCl₃ complexes above, since the primary distortion concerned a change from planarity to trigonal pyramid. But the geometrical distortion in the ZCl₄ units is more drastic, taking them from a see-saw to a square pyramidal shape. But the overarching theme here is the strong binding of the two anions.

The strength of this dative bonding is also evident in the gas phase energetics. Although the binding energies remain positive, and so are connected with a 22–29 kcal/mol energy barrier for dissociation, the interaction energies are negative for these complexes, even in the gas phase. This strong binding is in part due to very large negative electrostatic energy components, on the order of -100 kcal/mol. This observation may seem at first sight counterintuitive, given the interaction occurs between a pair of anions. But it must be understood that the electrostatic interaction term is far more complicated than a simple ion-ion term when the two subunits lie close to one another, involving a full treatment of the entire electron cloud of each species.

As an interesting probe of the electrostatic interaction, the long distance picture would of course be purely ion-ion repulsive. However, upon closer approach this ion-ion approximation breaks down and the more complete treatment of the interactions between the electron clouds changes quite a bit. The electrostatic component of the interaction energies in each of the complexes can be seen in the penultimate column of Table 1 to be attractive in many cases, and in fact quite a bit so in some. So despite an initial repulsive force at long distance, the Coulombic phenomena can be rather attractive as the two anions approach one another. And this attraction can arise even though the maximum of the molecular electrostatic potential in the Lewis acid is negative, as witness the last column of Table 1.

All in all, as we proceed from 2A to 2B metals and then to 5A pnicogens, there seems to be a steady progression to a heavier proportion of covalent/dative bond to the C of CN^- .

One might be initially surprised that a distinctly endothermic process like the gas-phase association of the CN⁻ with some of these other anions, may represent a metastable equilibrium, with a substantial energy barrier separating the complex from the much more stable isolated anions. However, this sort of behavior is not all that uncommon. In fact, it seems to be a common feature of the dissociation of other anion-anion complexes including H-bonds [31–36] and halogen bonds [37–41], as well as other sorts of species [42]. Regarding the height of the energy barrier, it is

typically below 10 kcal/mol or so for H-bonded complexes between ions of like charge [43–46], a bit higher at 15 kcal/mol for the $(H_2PO_4^-)_2$ dimer [47] or for a pair of anions terminating in carboxyl groups [33]. These barriers climb up above 20 kcal/mol for $CN^-\cdots MCl_3^-$ complexes with M a member of group 2A of the periodic table, i.e. Be, Mg, etc. [28] and higher still [29], more than 25 kcal/mol when M is a transition metal from group 2B:Zn, Cd, and Hg. The barriers increase further, up near 30 kcal/mol for the pnicogen bonded complexes [30] and certain others [32].

1.1.2. Multiple CN⁻ ligands

Because of the strength with which CN binds to an electrophile, one might wonder whether more than one such anion can simultaneously engage in a complex. A ZF3 species, where Z refers to one of the pnicogen atoms P, As, Sb, or Bi, contains three σ -holes, one opposite each Z-F covalent bond. So in principle, it would be possible for three nucleophiles like CN- to engage in a dative bond with the central Z. Calculations [48] compared the binding of CN⁻ to neutral species NH₃ and NCH, both of which interact with the Z via their N atom. In keeping with its strong nucleophilic character, CN^- engages in a stronger and shorter bond (see Fig. 2a) than either of the two neutral bases. For example, the $R(C \cdot \cdot \cdot P)$ distance in $NC^- \cdot \cdot \cdot PF_3$ is only 1.863 Å, and its binding and interaction energies are -22.7 and -77.7 kcal/mol, respectively. These properties far outweigh the bond distance and energetics for the two neutral N-bases. Given their bond critical point densities in the 0.08–0.13 au range, there is some grounds for attributing at least partial covalent character to all of these NC-...ZF₃ complexes.

All three of these bases can engage in a pair of pnicogen bonds with the central Lewis acid simultaneously. But there is an exception. The two smaller pnicogen atoms P and As are unable to hold two CN⁻ anions at the same time. And even for SbF₃ and BiF₃ which are capable of holding two CN⁻ anions, as seen in Fig. 2b, the energetics are not strong. The interaction energies are -4.3 and -12.9 kcal/mol, respectively, healthy quantities. But the binding energies, which also take into account the monomer deformation energies, are quite small, even positive for Z = Sb. These relatively poor binding energies are due to the fact that the second CN⁻ anion must interact with a ZF₃-CN⁻ complex that already holds a full negative charge. And as shown in the earlier section, such complexes involving a pair of anions represent only metastable equilibria. So it is possible for Z to engage in two dative pnicogen bonds, but i) only with the heavier Z atoms and ii) only to form metastable equilibrium complexes. It should be added as well that the bond critical point densities for these double pnicogen bonds are quite a bit smaller than for the single bonds, only about 0.04 au, so do not have much covalent bond character.

Both the weaker NH_3 and NCH bases were also able to engage in a pair of pnicogen bonds [48] with all of the ZF_3 species tested, and all with negative binding and interaction energies. While NCH is

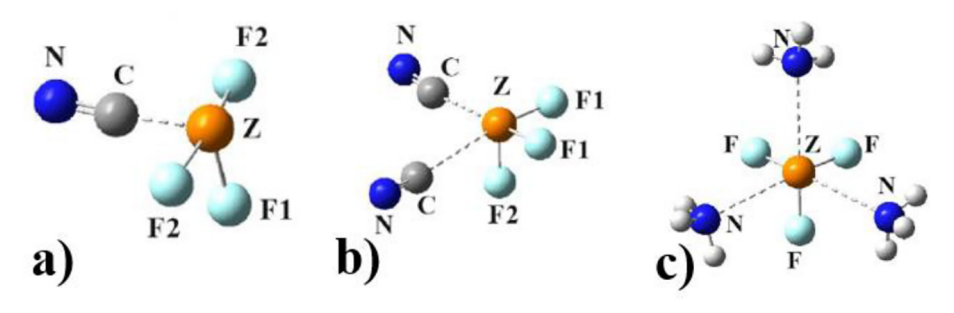


Fig. 2. Geometries of ZF₃ bound to a) 1 and b) 2 CN⁻ anions, and c) three NH₃ molecules.

too weak a base to engage in three simultaneous pnicogen bonds, such an arrangement is possible for NH_3 , with a structure exhibited in Fig. 2c. In summary, the full charge of CN^- is both a virtue and a vice. The charge makes for a very strong dative pnicogen bond with a first anion. But at the same time, the charge that it has added to the ZF_3 - CN^- complex repels the approach of a second CN^- , making it difficult to engage in a second such interaction.

The extreme nucleophilicity of the CN- anion can also induce other atoms to engage in multiple noncovalent interactions. As an example, each of the series of triel atoms Tr were situated as a TrF₂ group on a naphthalene ring system [49]. Not unexpectedly, a CN⁻ anion is able to engage in a Tr···C triel bond with any of the triel set B, Al, Ga, In, and Tl. This bond can be rather short, as for example $R(B \cdot \cdot \cdot C) = 1.643$ Å so can be fairly represented as a dative bond to the C of CN⁻. But what was of especial interest was the fact that this same bond persists even if the Tr atom is already engaged in an internal Tr bond with a NH₂ group on a neighboring C^{α} atom of the naphthalene. The $R(Tr \cdot \cdot \cdot C)$ bond is barely elongated by this second interaction. Taking B as an example, the stretch is only 0.015 Å, and for the largest Tr atom $R(T1 \cdots C)$ elongates by only 0.031 Å. The interaction energies in Table 2 confirm that there is little loss of bond strength. Using Tr = B as an example again, the interaction energy of CN⁻ with the naphthalene system diminishes from 85 to 79 kcal/mol if there is an internal NH₂ group already interacting with the B atom. So the presence of a second, internal, triel bond does not appear to appreciably weaken the primary dative bond to the C of CN-.

1.1.3. Multiple surrounding electrophiles

Besides other anions and pnicogen atoms, the CN- anion can also engage in strong interactions with a host of other electrophiles. A recent set of calculations [50] considered interactions with a variety of ligands that allowed for H-bonding (HF and HCl) as well as halogen, chalcogen, pnicogen, tetrel, and triel bonds. Some of the geometries associated with these interactions are illustrated in Fig. 3. A pair of HF molecules donate a proton to both the C and N ends of CN⁻, that together amounted to a total binding energy of 52 kcal/mol for the FH···CN-···HF trimer. When surrounded by two HCl molecules, the one on the C end actually transferred its proton over to the CN⁻ species, leaving the full cluster as ClH···NCH···Cl-. A similar transfer occurred with the halogen bonding FCl ligands, leading to a FCl···NCCl···F- unit, whereas no such transfer occurred with a pair of FBr ligands. An apparently strong dative bond to the C occurs with a pair of chalcogen-bonding SF₂ units. The S that is located on the C end of CN is only some 1.928 Å from the C, close to a covalent bond length. The heavier Se atoms of SeF₂, on the other hand, maintain a slightly longer distance, more akin to a strong noncovalent bond. The C and N ends of CN behave more similarly when a pair of pnicogenbonding PF₃ or AsF₃ ligands are added. On the other hand, the Si and Ge tetrel atoms of TF4 come very close to the C and N atoms, right around 2.0 Å, in what appears to be nearly covalent dative bonding. A very similar situation is seen for the triel atoms Al and Ga in TrF₃.

The addition of a third H-bonding HF molecule attaches itself to the N end of CN⁻, while HCl again transfers a proton across to the C atom, leaving a $(HCl)_2\cdots NCH\cdots Cl^-$ configuration. FCl again transfers its Cl atom to the C of CN^- even when there are two ClF molecules connected to the N atom. FBr does not fully transfer its Br atom to C, but places it roughly midway between the C and the F, suggesting at least a partial dative C-Br bond. A pair of SF_2 or SeF_2 molecules adhere to the N end of CN^- , leaving the third engaged in a chalcogen bond with the C, too long to be considered dative. A similar arrangement is observed with three PF_3 or ASF_3 molecules. The tetrel-bonding ligands again approach closely enough that some covalency can be concluded. The situation is not much changed when the number of ligands is increased up to 4.

It would appear, then, that clustering of a number of electrophilic ligands around the CN⁻ species leads to some interesting phenomena. In some cases, there is a full or partial transfer of an atom across to the C atom. In others, the ligand is close enough to the C that a partially covalent dative bond would appear to best categorize it. But as a bottom line, the fact that an anion like CN⁻ can surround itself with multiple electrophilic ligands is not a surprise, just as numerous other anions behave in a similar way [51,52].

Of course, clustering via halogen and related bonds does not require a central anion. Pnicogen bonding is present in the structures of (PH₂F)_n and (PH₂Cl)_n clusters [53] and aggregates [54] of NH₃, PH₃, and PFH₂. Halogen and hydrogen bonds in tetrameric mixed clusters of HF and FCl [55] are responsible for ring structure. Another work [56] examined halogen bonds in one-dimensional NCX clusters as large as 10 units (X = Cl and Br) with any eye toward cooperative effects. With regard to a central molecule within a cluster, the halogen bonds that stabilize Cl₂ and Br₂ within cages of water molecules [57] have been examined, as have interactions of a halide ion with neutral molecules via HBs, XBs, or related noncovalent bonds [58]. Efforts [59–71] are ongoing to design receptors that bind to halides and other anions via XBs, YBs, ZBs, and even tetrel bonds (Si,Ge family) via dipodal pairs of such bonds.

1.2. MeCH₂ Anion

Another sort of anion in which the C atom is the primary electron donor atom would be a derivative of an alkane, from which a proton has been removed. An example would be $CH_3CH_2^-$, whose MEP is shown in Fig. 4. Note the strong red area near the CH_2 group, coincident with the lone pair of the C from which the proton of ethane has been extracted. The value of the minimum of this MEP on the ρ = 0.001 au isodensity surface is -143.0 kcal/mol [72]. This C is prime to donate its lone pair to another molecule in what would be a dative bond.

One of the more interesting scenarios would pair this C lone pair with a tetrel atom on another molecule. In order to maximize this interaction, a highly electron-withdrawing F atom was placed on the tetrel atom so as to enhance its positive σ -hole, and thereby maximize the interaction between the two units [72]. An example of such a complex is pictured in Fig. 5 which pairs CH₃CH $_2^-$ with H₃FGe as a particular example. The distance between each T atom and C of CH₃CH $_2^-$ is displayed in the first column of Table 3, which

Table 2Distances (Å) from C of CN⁻ to Tr atom, and interaction energy (kcal/mol) between CN⁻ and naphthalene system, calculated at the MP2/aug-cc-pVDZ level.

	$R(Tr \cdot \cdot \cdot C)$	E _{int}		$R(Tr\!\cdots\!C)$	E _{int}
$C_{10}H_7BF_2$	1.643	-85.31	$C_{10}H_9NBF_2$	1.658	-78.98
$C_{10}H_7AlF_2$	2.025	-88.08	$C_{10}H_9NAlF_2$	2.067	-67.21
$C_{10}H_7GaF_2$	2.015	-86.32	C ₁₀ H ₉ NGaF ₂	2.017	-90.11
$C_{10}H_7InF_2$	2.204	-83.68	$C_{10}H_9NInF_2$	2.222	-77.54
C ₁₀ H ₇ TIF ₂	2.205	-76.72	$C_{10}H_9NTIF_2$	2.236	-72.50

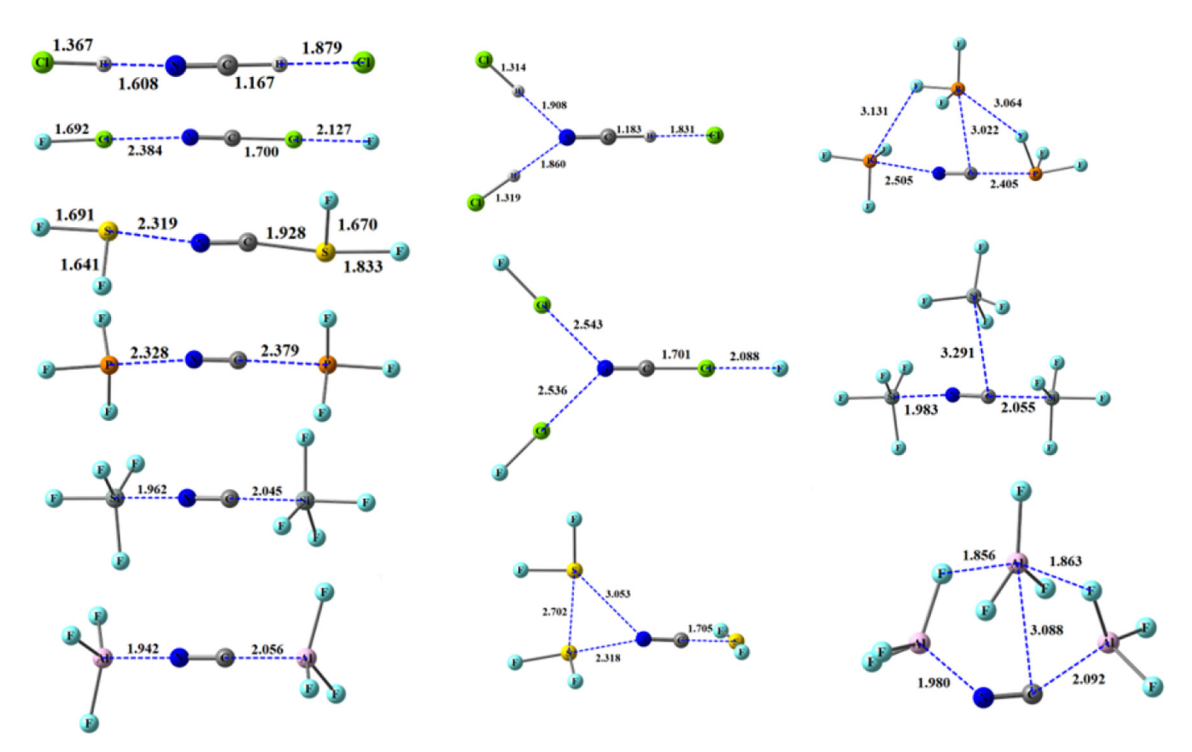


Fig. 3. Geometries of selected clusters of CN⁻ at the M06-2X/aug-cc-pVDZ level. Distances in Å.

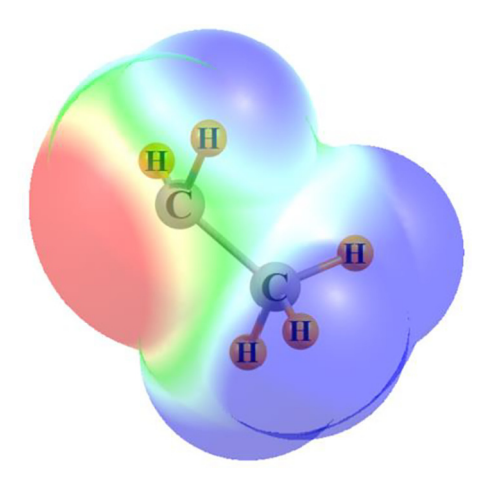


Fig. 4. Molecular electrostatic potential surrounding $CH_3CH_2^-$ anion at the MP2/aug-cc-pVDZ level. Red and blue regions correspond to negative and positive potentials, respectively. ((Colour online.))

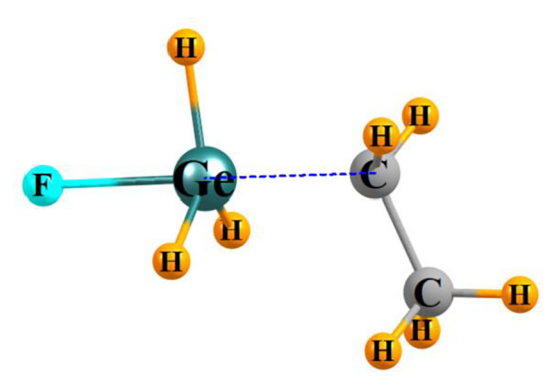


Fig. 5. Geometry of complex between H₃FGe with CH₃CH₂.

Table 3

T—C bond length (Å) in complexes of TH $_3$ F with CH $_3$ CH $_2$, and the ratio of this distance to the sum of the T and C covalent radii, along with bond critical point parameters (au) and interaction and binding energies (kcal/mol). Quantities computed at the MP2/aug-cc-pVDZ level of theory.

	$R(T \cdot \cdot \cdot C)$	%cov	ρ	Н	E _{int}	E _b
SiH ₃ F	2.013	108	0.087	-0.038	-86.9	-56.5
GeH₃F	2.083	106	0.098	-0.050	-87.5	-57.1
SnH₃F	2.277	106	0.079	-0.025	-88.4	-64.7
PbH ₃ F	2.356	106	0.077	-0.021	-83.6	-61.1

is rather short, between 2.0 and 2.4 Å. More importantly, these distances are only slightly longer than the sum of the covalent atomic radii, indicated by the 106–108% of this sum in the next column of Table 3. Another verification of their covalent character arises from the AIM analysis. The bond critical point densities are right around 0.1 au, with clearly negative values of H.

The energetics of the complexation are also highly suggestive of a dative covalent bond. The interaction energies are just shy of 90 kcal/mol, in the covalent bond range. Following incorporation of the deformation of the two monomers, the binding energies in the last column of Table 3 are also quite large, between 57 and 65 kcal/mol. These sorts of interactions are supported by an earlier survey [73] of crystal data, along with calculations of model systems, but which were limited to Sn···Sn bonds, with no consideration of C.

1.3. Neutral Base Molecules

Although CN⁻ and carbanions are of course strong nucleophiles, neutral molecules too can participate in related sorts of bonding. In fact, there is no prerequisite that the C have available a lone electron pair.

1.3.1. CH₃M

Consider for example, methane with a metal substituent like CH₃Li. As seen in Fig. 6b, the Li atom donates charge to the rest

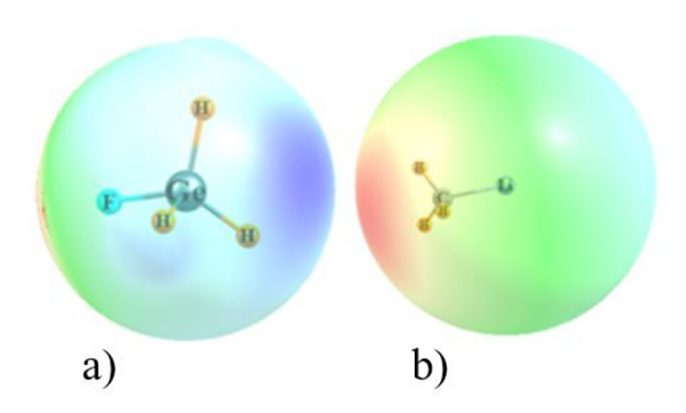


Fig. 6. Molecular electrostatic potential surrounding a) H_3FG and b) CH_3Li at the M06-2X/aug-cc-pVDZ level. Blue areas indicate most positive potential, most negative is indicated in red. ((Colour online.))

of the molecule, so builds up a negative region along the Li-C bond extension, between the three H atoms. A fluorinated molecule such as H_3FGe contains a positive $\sigma\text{-hole}$ lying along the F-Ge bond extension, shown in blue in Fig. 6a. So there will be a natural electrostatic attraction between these two molecules, that can result in a $Ge\cdots C$ interaction.

Table 4 shows [74] that the C does not approach close enough to the tetrel atom on its partner subunit than 3 Å, much too long to contain covalent character. The density at the bond critical point is quite small as well, only 0.01 or less, far below the threshold for a covalent bond. The energetics of these complexes are listed in the last two columns. Interaction energies range between 2.9 and 10.1 kcal/mol, which constitute healthy noncovalent bonds but below the threshold for a covalent bond.

The bonding can be strengthened by exchanging the Li for the progressively more electropositive Na and K. Taking the bond between a pair of Ge atoms in H₃FGe···GeH₃M as a sample, the change of metal atom M from Li to Na and then to K raises E_{int} from 4.8 to 5.5 and then to 6.9 kcal/mol. However, even in this Ge···Ge case, the interaction would not be classified as covalent or dative.

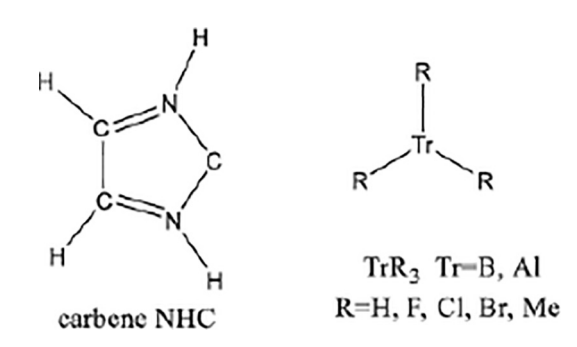
In fact, it might be noted that the CH_3Li base does not contain any lone pairs on the C atom. The charge transfer from this base derives instead from the three C—H bonding orbitals. This lack of a lone pair can be taken as one rationale for the failure to engage in a partially covalent bond. The idea that the electron donor source of the tetrel-bonding base can be a bonding orbital is not entirely without precedent. For instance, H_3FT can accept electron density [75] from the $\sigma(MH)$ bonding orbital of LiH, NaH, BeH₂ or MgH₂. A more recent example refers to the SiH₅⁺ and GeH₅⁺ cations which [76] contain a tetrel bond between TH_3^+ and the $\sigma(HH)$ bonding orbital of H_2 . In a broader context, the C—C pseudo- π bonding orbital of cyclopropane has been suggested [77] as the electron source in a halogen bond with FCl, and a similar idea [78] applies to a P—P bond of P_4 .

Table 4 T—C bond length (Å) in complexes of TH_3F with CH_3Li and bond critical point density (au) and interaction and binding energies (kcal/mol). Quantities computed at the MP2/aug-cc-pVDZ level of theory.

	$R(T \cdot \cdot \cdot C)$	ρ	E _{int}	E _b
CH ₃ F	3.344	0.0057	-2.89	-2.85
SiH₃F	3.244	0.0087	-5.69	-5.35
GeH₃F	3.224	0.0095	-6.84	-6.35
SnH ₃ F	3.162	0.0125	-10.06	-8.85
PbH₃F	3.225	0.0124	-10.11	-9.27

1.3.2. Carbenes

In addition to being an atom on an anion, a C atom can participate in a dative bond as a carbene moiety. The carbene C atom of a modified imidazole species as pictured below was allowed to interact [79] with the central Tr atom in each of the various forms of TrR₃.



As one might expect, the $\pi\text{-hole}$ lying directly above the Tr atom in the planar TrR_3 monomers is most positive for the most highly electron-withdrawing R substituents F > Cl > Br > Me, with H situated midway between F and Cl. Replacement of B by its more electropositive Al Tr atom raises the intensity of the $\pi\text{-hole}$ as well. As indicated in Fig. 7 there is a fairly strong negative region of the MEP near the C atom of NHC, coincident with the C lone pair, with a minimum MEP value of -0.083 au. Replacement of the C by Si cuts the value of this minimum in half. There are smaller reductions in its value if two of the H atoms of NHC are replaced by F, either on the C or N atoms.

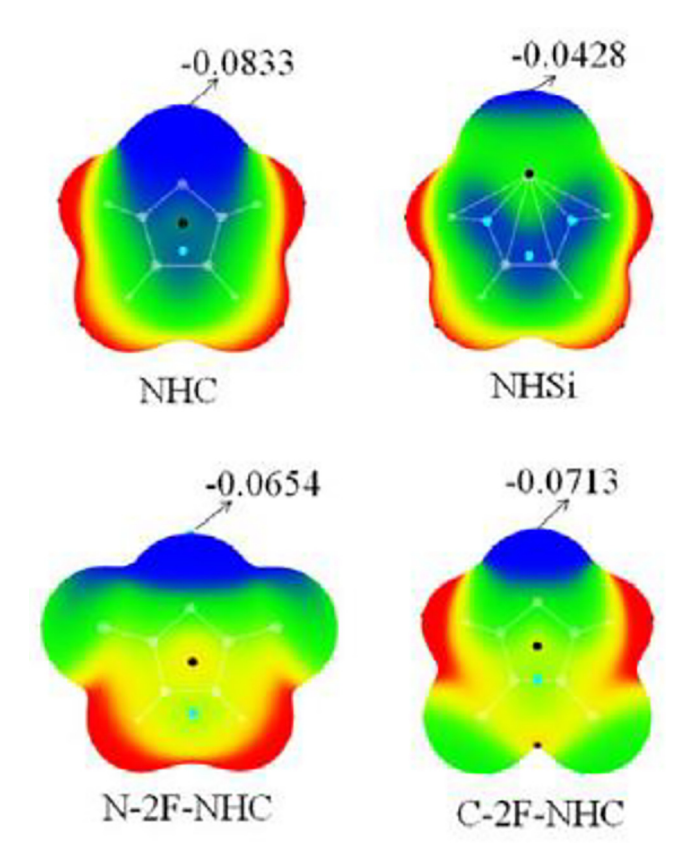


Fig. 7. Molecular electrostatic potential surrounding indicated molecules at the MP2/aug-cc-pVDZ level. Blue areas indicate most negative potential, most positive is indicated in red. Values of the maxima are displayed in au. ((Colour online.))

The R(C···Tr) bond lengths of the putative dative bonds are displayed in the first column of Table 5. The C···B distances are all quite short, on the order of 1.6 Å, consistent with its classification as a partially covalent dative bond. This categorization is buttressed by AIM bond critical point densities that exceed 0.1 au, and with negative values of energy density H. The corresponding C···Al bond lengths are a bit longer, roughly 2.0 Å, commensurate with the larger atomic radius of Al. Their critical point densities are a bit below the 0.1 au threshold for covalency but their values of H are also negative, so are on the border of a covalent dative bond. One might also note that there appears to be some relationship between the intermolecular distances and some of the AIM quantities. Indeed, the density at the bond critical point grows uniformly as the bond is shortened. A linear correlation between R (C···Tr) and $\rho_{\rm BCP}$ is characterized by a correlation coefficient R² of 0.95.

The last two columns of Table 5 show that these bond energies are quite large, higher than a typical noncovalent bond. The interaction energies for the C···B bonds range all the way up to 88 kcal/mol, bordering on covalent quality. Even though the C···Al interaction energies are a bit smaller, some of them reach up to 70 kcal/mol. Due to a certain amount of deformation energy for the monomers, the binding energies are a bit smaller, but still higher than a typical noncovalent bond.

The ability of carbenes to serve as electron donor in bonds of this type are fairly well established. They have been shown to do so in pnicogen and tetrel bonds [80–86], as well as halogen [87–91] and chalcogen bonds [92].

1.3.3. π -Systems

In addition to a lone pair, or several σ -covalent bonds, another pocket of electron density from which C atoms might donate electrons would be a π -system, as might occur in an alkene for example. Taking simple ethylene as a starting point, the π -cloud could offer density to an approaching Lewis acid, as for example in participating in a pnicogen bond with ZCl₃, where Z could be P, As, or Sb [93]. The pnicogen bond involves transfer from the π (CC) molecular orbital to a σ *(ZCl) antibond. As indicated in the first three rows of Table 6, the Z atom approaches to within about 3.2 Å of one of the two ethylene C atoms. The interaction energy is between 3 and 5 kcal/mol, and the bond critical point density is between 0.010 and 0.015 au, solidly in the range of a noncovalent bond.

Replacing the four H atoms by highly electron-withdrawing substituents such as F or CN would drain some of the density from the π -system, inhibiting the ability of an approaching electrophile to acquire density from this area. These effects are evident in the MEP maps of the three ethylene derivatives in Fig. 8, where the

region above the ethylene π bond changes its extremum from negative -0.027 au to positive + 0.072 au for the cyano-derivative.

Although these changes in the potential would suggest a weaker interaction with the ZCl_3 electrophile, the last six rows of Table 6 show very little reduction in the interaction energy, and in fact a larger energy for $C_2(CN)_4$. The critical point densities, however, indicate that the $Z\cdots C$ bond is slightly weaker than for the unsubstituted ethylene. So it would appear that even though the pnicogen bond weakens with these substitutions, as expected from simple principles, the total interaction energy is able to maintain itself and even strengthen.

The explanation of this apparent paradox stems from consideration of the overall geometry and the introduction of secondary bonds. As is evident in Fig. 9, not only does the (orange) Z atom approach one of the C atoms of ethylene, but one or more of the Cl atoms of ZCl_3 approach within bonding range of the other C, or in some cases to one of the atoms of the substituent. The last column of Table 6 shows that this secondary interaction can be fairly strong, with critical point densities nearly as large as that between Z and C. It must also be borne in mind that the values in the last column should effectively be doubled as there are two such secondary interactions. So the primary pnicogen... π bond is reasonably strong, but nowhere near covalent bond stature, and is generally supplemented by subsidiary noncovalent bonds involving the Cl atoms of ZCl_3 .

In addition to pnicogen bonds, chalcogen atoms are also inclined toward C=C π -systems as electron sources. Calculations considered both SF₂ and SF₄ as Lewis acids [94]. They were each paired with HC=CH, H₂C = CH₂, H₂C = CH-CH = CH₂ (both cis and trans) and benzene as a fully aromatic system. The geometries of the complexes are presented in Figs. 10 and 11, for SF₂ and SF₄, respectively, and show the S atom comes within about 3 Å of the

Table 6 Z—C bond length (Å) in complexes of R_2C = CR_2 with ZCl_3 and bond critical point density (au) and interaction energy (kcal/mol), at the MP2/aug-cc-pVDZ level of theory.

	$R(Z{\cdot}\cdot{\cdot}C)$	$\rho(Z\!\!\cdot\!\cdot\!\cdot\!C)$	E_{int}	$\rho(Cl\!\cdot\cdot\cdot R^a)$
$C_2H_4\cdots PCl_3$	3.341	0.0095	-2.93	0.0048
$C_2H_4\cdots AsCl_3$	3.249	0.0124	-3.71	0.0046
$C_2H_4\cdots SbCl_3$	3.225	0.0151	-4.70	0.0046
$C_2F_4\cdots PCl_3$	3.201	0.0107	-2.54	0.0063
$C_2F_4\cdots AsCl_3$	3.210	0.0114	-2.36	0.0066
$C_2F_4\cdots SbCl_3$	3.294	0.0118	-2.17	0.0066
$C_2(CN)_4 \cdot \cdot \cdot PCl_3$	3.230	0.0098	-5.90	-
$C_2(CN)_4 \cdot \cdot \cdot AsCl_3$	3.353	0.0077	-5.45	0.0063
$C_2(CN)_4$ ··· SbCl ₃	3.491	0.0068	-5.23	0.0061

^a R = F atom for C_2F_4 and C atom of CN for $C_2(CN)_4$.

Table 5 Intermolecular distance (Å), AIM properties (au), and energetics (kcal/mol) in complexes of carbenes with TrR₃, at the MP2/aug-cc-pVDZ level of theory.

Complexes	$R(C \cdot \cdot \cdot Tr)$	ρ	$\nabla^2 \rho$	Н	E _{int}	E _b
NHC···BH ₃	1.593	0.144	0.380	-0.119	-74.16	-55.20
NHC···BF ₃	1.659	0.140	0.136	-0.127	-73.62	-37.50
NHC···BCl ₃	1.602	0.164	0.656	-0.159	-86.55	-53.51
NHC···BBr ₃	1.590	0.168	0.672	-0.165	-88.25	-58.43
NHC···AIH ₃	2.027	0.058	0.284	-0.006	-50.18	-42.56
NHC···AlF ₃	2.042	0.065	0.312	-0.010	-68.33	-55.47
NHC···AlCl ₃	2.027	0.070	0.328	-0.013	-70.44	-57.67
NHC···AlBr ₃	2.020	0.071	0.336	-0.013	-69.82	-57.87
N-2F-NHC···BH ₃	1.594	0.135	0.452	-0.104	-58.49	-41.71
N-2F-NHC···AlH ₃	2.131	0.049	0.248	-0.003	-35.06	-29.55
C-2F-NHC···BH ₃	1.591	0.143	0.404	-0.117	-70.83	-52.53
C-2F-NHC···AlH ₃	2.088	0.065	0.280	-0.006	-46.57	-39.58
N-2F-NHC···BMe ₃	1.634	0.123	0.428	-0.089	-44.65	-22.50
N-2F-NHC···AlMe ₃	2.152	0.046	0.236	-0.002	-30.96	-25.22

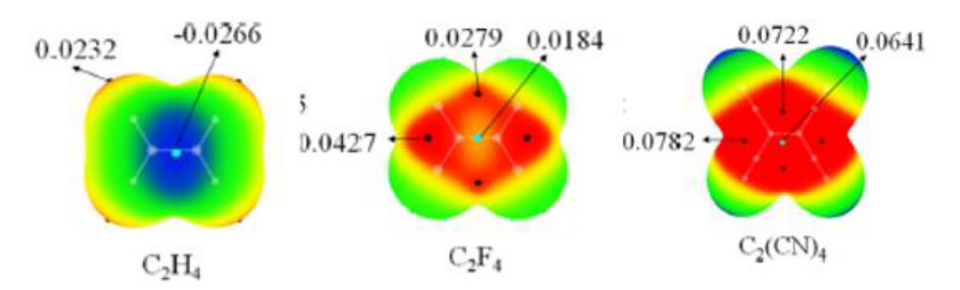


Fig. 8. Molecular electrostatic potential surrounding indicated molecules at the MP2/aug-cc-pVDZ level. Red areas indicate most positive potential, most negative in blue. Values of the maxima are displayed in au. ((Colour online.))

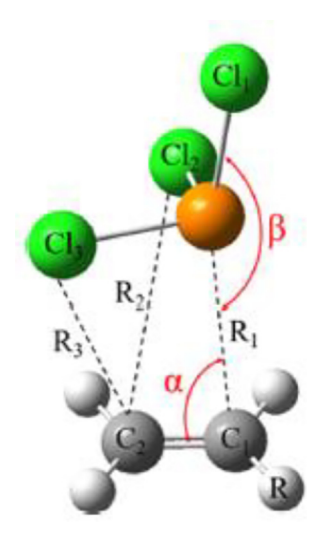


Fig. 9. Arrangement of complexes pairing $R_2C = CR_2$ with ZCl_3 , defining geometrical parameters.

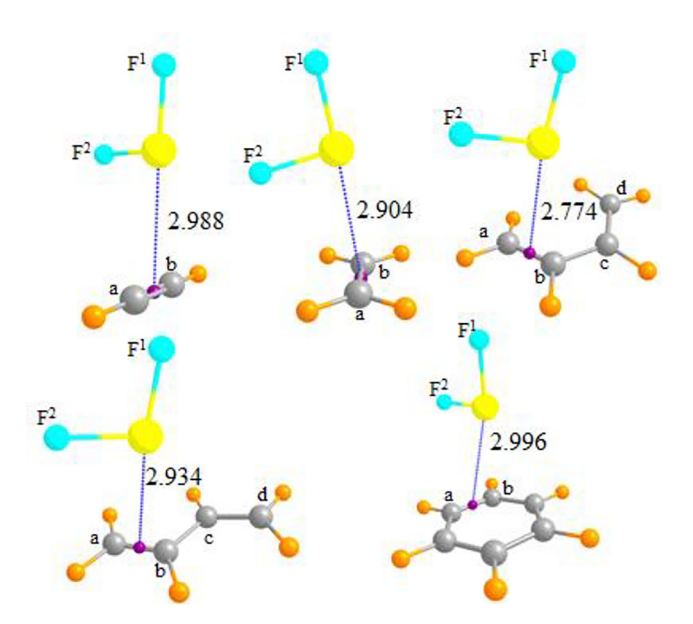


Fig. 10. Optimized geometries of SF_2 with ethyne, ethylene, *cis*-butadiene, *trans*-butadiene, and benzene at the MP2/aug-cc-pVDZ level. Distances in Å. Small purple sphere represents midpoint of indicated bond. ((Colour online.))

pertinent C—C midpoint, shown by purple spheres. These distances are a bit shorter for SF_2 than for SF_4 .

The binding energies of these various complexes are displayed in Table 7 where it may be noted first that SF_2 and SF_4 bind with

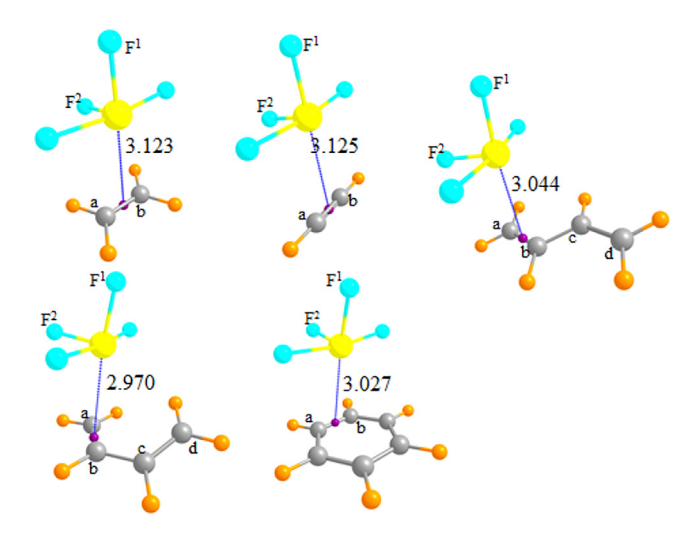


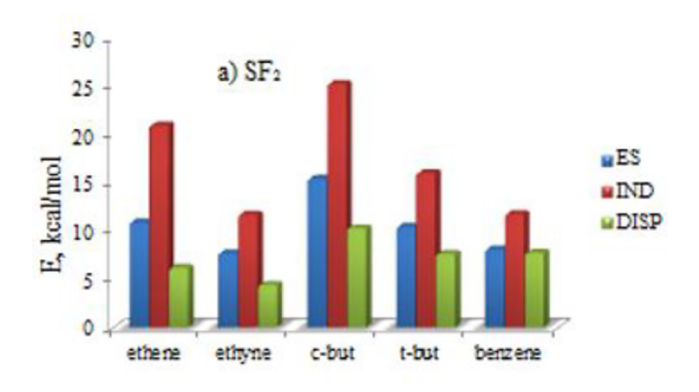
Fig. 11. Optimized geometries of SF_4 with ethyne, ethylene, *cis*-butadiene, *trans*-butadiene, and benzene at the MP2/aug-cc-pVDZ level. Distances in Å. Small purple sphere represents midpoint of indicated bond. ((Colour online.))

roughly equal power, generally within about 1 kcal/mol of one another. With the exception of benzene, it is SF_2 which engages in the stronger bond, and it is its complex with \emph{cis} -butadiene which is strongest of all, at 6.6 kcal/mol. Nonetheless, these bonds are far weaker than would meet the criterion for a covalent bond, which is supported by the AIM bond critical point densities in the last two columns of Table 7, all well below 0.1 au.

A new wrinkle thrown into these interactions by the involvement of π -systems is a second type of charge transfer. A standard noncovalent bond transfers charge from the base lone pair into the σ^* antibond of the Lewis acid. The same is true here, except that it is the π orbital that substitutes for the donor lone pair. But another type of transfer occurs here as well. Some charge transfers in the other direction, from the S lone pairs to the π^* antibonding orbitals of the alkene. These two transfers are thus in opposite directions,

Table 7 Binding energies (kcal/mol) and bond critical point density (au) in complexes of indicated π -system with SF₂ and SF₄, at the MP2/aug-cc-pVDZ level of theory.

	Еь		ρ_{BCP}	ρ_{BCP}		
	SF_2	SF ₄	SF ₂	SF ₄		
Ethene	4.13	3.31	0.0165	0.0125		
Ethyne	3.67	3.51	0.0134	0.0117		
c-But	6.61	5.18	0.0214	0.0170		
t-But	5.05	4.43	0.0171	0.0153		
Benzene	4.55	5.50	0.0137	0.0141		



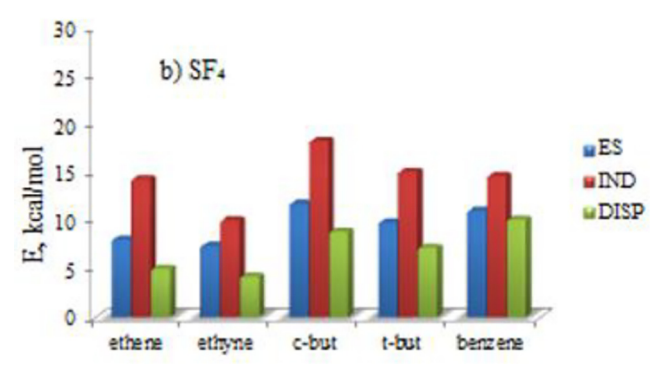


Fig. 12. Attractive SAPT components of interaction energies of π -systems with a) SF₂ and b) SF₄ computed with the aug-cc-pVDZ basis set. ES = electrostatic, IND = induction, DISP = dispersion.

so are able to amplify one another to a certain extent, while also lowering the total transfer from either molecule to the other.

One interesting feature of noncovalent bonds involving π -donation is the importance of induction/polarization energy. Most noncovalent bonds, including H-bonds, that employ a lone pair as the source of charge donation from the Lewis base are heavily dependent on electrostatic attraction. However, as may be seen in Fig. 12, it is induction (IND) which plays the chief role in these π -donor systems, making a contribution that is nearly double that of electrostatics (ES). Another distinguishing characteristic of these π -donor systems is the unusually large contribution from dispersion (DISP) which is nearly as large as ES. As a last point, there is a weak linear relationship between the ES and IND components and the value of the bond critical point density, with correlation coefficients on the order of 0.8 for both.

In summary, π -systems are competent to engage in reasonably strong noncovalent bonds with Lewis acids of both pnicogen and chalcogen type. Along with the use of π -orbitals as chief donors to the σ^* orbitals of the acid, there is a transfer in the opposite direction, from lone pairs of the Lewis acid to the π^* orbitals of the nominal base. Altogether, these effects lead to an amplified importance of charge transfer and induction phenomena, as well as a larger dispersion contribution. Nevertheless, these bonds are far weaker than a covalent dative bond, falling more in line with standard noncovalent interactions.

2. Summary

There are a number of C-containing entities which can act as Lewis bases. Chief among them, and the most powerful due to its overall negative charge and compact size, is the CN⁻ anion. The C atom contains a lone pair (as does the N) which can be donated to a Lewis acid in a noncovalent bond that can be strong enough to be termed covalent and dative. Even if the acid unit is anionic,

the C lone pair can overcome the long-range ion-ion repulsion to approach close enough to engage in a strong bonding interaction. This same short-range ion-ion attraction enables two CN^- anions to engage in bonding interactions with a neutral molecule. The CN^- anion is not limited to interaction with a single partner, but can serve as a central ion surrounded by a number of ligands that interact through a host of different types of bonds, including H, halogen, chalcogen, pnicogen, tetrel, and triel bonds. In certain situations, a H or Cl atom can transfer across to the C from the neighboring ligand. Another anion whose C lone pair can be donated to another molecule is the $MeCH_2^-$ carbanion. One sort of example is the tetrel bond this anion forms with a neutral H_3FT molecule, where T can be any of a series of tetrel atoms.

Although the interactions are not as strong, and less covalent, there are also neutral C-containing molecules which can function as Lewis base. Despite the absence of any C lone pair, CH₃M units can donate electron density from their σ -bonding orbitals to a neutral H₃FT in a ditetrel bond, closely analogous to the well-studied dihydrogen bond. Carbenes, too, contain a C lone pair that can be donated to another unit. Some of these can be quite strong, within the covalent range. Another primary source of electron density associated with C atoms is the π -system of alkenic or aromatic molecules. Generally weaker than the interactions arising from C lone pairs, these π -complexes typically involve a magnified degree of dispersion energy.

The sorts of C-electron donors discussed above are not meant as an exhaustive list. For example, the C atoms of an aromatic group can donate electrons to cations that are situated above the π -system [95–97]. As another example, enolates can be stabilized by anion $\cdots \pi$ or π -hole interactions [98].

Declaration of Competing Interest

The authors declare that they have no known competing financial interests or personal relationships that could have appeared to influence the work reported in this paper.

Acknowledgement

This material is based upon work supported by the National Science Foundation under Grant No. 1954310.

References

- G.C. Pimentel, A.L. McClellan, The Hydrogen Bond, Freeman, San Francisco, 1960.
- [2] S.N. Vinogradov, R.H. Linnell, Hydrogen Bonding, Van Nostrand-Reinhold, New York, 1971.
- [3] M.D. Joesten, L.J. Schaad, Hydrogen Bonding, Marcel Dekker, New York, 1974.
- [4] P. Schuster, G. Zundel, C. Sandorfy, The Hydrogen Bond. Recent Developments in Theory and Experiments, in, North-Holland Publishing Co., Amsterdam, 1976.
- [5] O. Hassel, Science 170 (1970) 497–502.
- [6] J.P.M. Lommerse, A.J. Stone, R. Taylor, F.H. Allen, J. Am. Chem. Soc. 118 (1996) 3108–3116.
- [7] F.H. Allen, J.P.M. Lommerse, V.J. Hoy, J.A.K. Howard, G.R. Desiraju, Acta Cryst., B 53 (1997) 1006–1016.
- [8] I. Alkorta, S. Rozas, J. Elguero, J. Phys. Chem. A 102 (1998) 9278–9285.
- [9] P.L. Wash, S. Ma, U. Obst, J. Rebek, J. Am. Chem. Soc. 121 (1999) 7973–7974.
- [10] A.C. Legon, Angew. Chem., Int. Ed. Engl. 38 (1999) 2686–2714.
- [11] A. Karpfen, J. Phys. Chem. A 104 (2000) 6871–6879.
- [12] P. Metrangolo, G. Resnati, Chem. Eur. J. 7 (2001) 2511–2519.
- [13] P. Auffinger, F.A. Hays, E. Westhof, P.S. Ho, Proc. Nat. Acad. Sci., USA 101 (2004) 16789–16794.
- [14] D. Swierczynski, R. Luboradzki, G. Dolgonos, J. Lipkowski, Eur. J. Org. Chem. 2005 (2005) 1172–1177.
- [15] R.E. Rosenfield, R. Parthasarathy, J.D. Dunitz, J. Am. Chem. Soc. 99 (1977) 4860–4862.
- [16] G.R. Desiraju, V. Nalini, J. Mater. Chem. 1 (1991) 201–203.
- [17] F.T. Burling, B.M. Goldstein, J. Am. Chem. Soc. 114 (1992) 2313–2320.
- [18] K.W. Klinkhammer, P. Pyykko, Inorg. Chem. 34 (1995) 4134–4138.
- [19] M. Iwaoka, S. Tomoda, J. Am. Chem. Soc. 118 (1996) 8077–8084.

- [20] P. Sanz, O. Mó, M. Yáñez, Phys. Chem. Chem. Phys. 5 (2003) 2942–2947.
- [21] S.J. Grabowski, Struct. Chem. 30 (2019) 1141-1152.
- [22] A. Bauzá, T.J. Mooibroek, A. Frontera, Angew. Chem. Int. Ed. 52 (2013) 12317-12321
- [23] X. García-Llinás, A. Bauzá, S.K. Seth, A. Frontera, J. Phys. Chem. A 121 (2017) 5371-5376.
- [24] W. Zierkiewicz, M. Michalczyk, S. Scheiner, Phys. Chem. Chem. Phys. 20 (2018) 8832-8841.
- [25] W. Zierkiewicz, M. Michalczyk, R. Wysokiński, S. Scheiner, Molecules 24 (2019) 376.
- [26] P. Politzer, J.S. Murray, T. Clark, Phys. Chem. Chem. Phys. 15 (2013) 11178-11189.
- [27] D. Mani, E. Arunan, Phys. Chem. Chem. Phys. 15 (2013) 14377-14383.
- [28] W. Zierkiewicz, R. Wysokiński, M. Michalczyk, S. Scheiner, ChemPhysChem. 21 (2020) 870-877.
- [29] R. Wysokiński, W. Zierkiewicz, M. Michalczyk, S. Scheiner, ChemPhysChem. 21 (2020) 1119-1125.
- [30] S. Scheiner, R. Wysokiński, M. Michalczyk, W. Zierkiewicz, J. Phys. Chem. A 124 (2020) 4998-5006.
- [31] L.M. Azofra, J. Elguero, I. Alkorta, Phys. Chem. Chem. Phys. 22 (2020) 11348-
- [32] M.O. Miranda, D.J.R. Duarte, I. Alkorta, ChemPhysChem. 21 (2020) 1052-1059.
- [33] R. Barbas, R. Prohens, A. Bauzá, A. Franconetti, A. Frontera, Chem. Commun. 55 (2019) 115-118.
- [34] F. Weinhold, Angew. Chem. Int. Ed. 56 (2017) 14577-14581.
- [35] I. Alkorta, I. Mata, E. Molins, E. Espinosa, Chem. Eur. J. 22 (2016) 9226–9234.
- [36] I. Mata, E. Molins, I. Alkorta, E. Espinosa, J. Phys. Chem. A 119 (2014) 183-194.
- [37] J.M. Holthoff, E. Engelage, R. Weiss, S.M. Huber, Angew. Chem. Int. Ed. 59 (2020) 11150–11157.
- [38] C. Wang, Y. Fu, L. Zhang, D. Danovich, S. Shaik, Y. Mo, J. Comput. Chem. 39 (2018) 481-487.
- [39] S.M. Chalanchi, I. Alkorta, J. Elguero, D. Quiñonero, ChemPhysChem. 18 (2017)
- [40] G. Wang, Z. Chen, Z. Xu, J. Wang, Y. Yang, T. Cai, J. Shi, W. Zhu, J. Phys. Chem. B 120 (2016) 610-620.
- [41] D. Quinonero, I. Alkorta, J. Elguero, Phys. Chem. Chem. Phys. 18 (2016) 27939-
- [42] D. Quiñonero, I. Alkorta, J. Elguero, ChemPhysChem. 21 (2020) 1597-1607.
- [43] S.R. Kass, J. Am. Chem. Soc. 127 (2005) 13098–13099.
- [44] I. Mata, E. Molins, I. Alkorta, E. Espinosa, J. Phys. Chem. A 119 (2015) 183–194.
- [45] R. Prohens, A. Portell, M. Font-Bardia, A. Bauzá, A. Frontera, Chem. Commun. 54 (2018) 1841-1844.
- [46] F. Weinhold, Inorg. Chem. 57 (2018) 2035-2044.
- [47] I. Mata, I. Alkorta, E. Molins, E. Espinosa, ChemPhysChem. 13 (2012) 1421-
- [48] R. Wysokiński, W. Zierkiewicz, M. Michalczyk, S. Scheiner, J. Phys. Chem. A 124 (2020) 2046-2056.
- [49] W. Zierkiewicz, M. Michalczyk, S. Scheiner, Molecules 25 (2020) 635.
- [50] S. Scheiner, M. Michalczyk, R. Wysokiński, W. Zierkiewicz, Chem. Phys. 530 (2020) 110590.
- [51] S. Scheiner, M. Michalczyk, W. Zierkiewicz, Chem. Phys. 524 (2019) 55-62.
- [52] S. Scheiner, M. Michalczyk, W. Zierkiewicz, Coord. Chem. Rev. 405 (2020) 213136.
- [53] M.D. Esrafili, M. Vakili, M. Solimannejad, Chem. Phys. Lett. 609 (2014) 37-41.
- [54] U. Adhikari, S. Scheiner, J. Chem. Phys. 135 (2011) 184306.
- [55] J.E. Del Bene, I. Alkorta, J. Elguero, J. Phys. Chem. A 122 (2018) 2587–2597.
- [56] M.D. Esrafili, N.L. Hadipour, Mol. Phys. 109 (2011) 2451–2460.
- [57] J.M. Guevara-Vela, D. Ochoa-Resendiz, A. Costales, R. Hernández-Lamoneda, Á. Martín Pendás, ChemPhysChem. 19 (2018) 2512-2517.
- [58] J.E. Del Bene, I. Alkorta, J. Elguero, Chem. Phys. Lett. 655-656 (2016) 115-
- [59] G. Sánchez-Sanz, C. Trujillo, J. Phys. Chem. A 122 (2018) 1369–1377.

- [60] S. Chakraborty, S. Maji, R. Ghosh, R. Jana, A. Datta, P. Ghosh, Chem. Commun. 55 (2019) 1506-1509.
- [61] S. Scheiner, Molecules 24 (2019) 227.
- [62] L.M. Lee, M. Tsemperouli, A.I. Poblador-Bahamonde, S. Benz, N. Sakai, K. Sugihara, S. Matile, J. Am. Chem. Soc. 141 (2019) 810-814.
- [63] J.Y.C. Lim, I. Marques, V. Félix, P.D. Beer, Chem. Commun. 54 (2018) 10851-10854
- S. Scheiner, Faraday Disc. 203 (2017) 213-226.
- [65] N.A. Semenov, D.E. Gorbunov, M.V. Shakhova, G.E. Salnikov, I.Y. Bagryanskaya, V.V. Korolev, J. Beckmann, N.P. Gritsan, A.V. Zibarev, Chem. Eur. J. 24 (2018) 12983-12991.
- [66] S. Scheiner, J. Phys. Chem. A 121 (2017) 3606-3615.
- [67] J.Y.C. Lim, P.D. Beer, New J. Chem. 42 (2018) 10472-10475.
- [68] J. Stoesser, G. Rojas, D. Bulfield, P.I. Hidalgo, J. Pasan, C. Ruiz-Perez, C.A. Jimenez, S.M. Huber, New J. Chem. 42 (2018) 10476-10480.
- A. Dreger, E. Engelage, B. Mallick, P.D. Beer, S.M. Huber, Chem. Commun. 54 (2018) 4013-4016.
- [70] L. Zhou, Y. Lu, Z. Xu, C. Peng, H. Liu, Struct. Chem. 29 (2018) 533-540.
- [71] S. Scheiner, Molecules 23 (2018) 1147-1155.
- [72] A. Grabarz, M. Michalczyk, W. Zierkiewicz, S. Scheiner, ChemPhysChem. 21 (2020) 1934-1944.
- [73] A. Franconetti, A. Frontera, Dalton Trans. 48 (2019) 11208-11216.
- [74] S. Scheiner, Phys. Chem. Chem. Phys. 22 (2020) 16606–16614.
- [75] Q.-Z. Li, H.-Y. Zhuo, H.-B. Li, Z.-B. Liu, W.-Z. Li, J.-B. Cheng, J. Phys. Chem. A 119 (2015) 2217-2224.
- [76] S.P. Gnanasekar, E. Arunan, J. Phys. Chem. A 123 (2019) 1168-1176.
- [77] K. Hinds, J. Holloway, A.C. Legon, J. Chem. Soc. Faraday Trans. 93 (1997) 373-
- [78] I. Alkorta, J. Elguero, J.E. Del Bene, Phys. Chem. Chem. Phys. 18 (2016) 32593-
- [79] Z. Chi, W. Dong, Q. Li, X. Yang, S. Scheiner, S. Liu, Int. J. Quantum Chem. 119 (2019) e25867.
- [80] H. Lin, L. Meng, X. Li, Y. Zeng, X. Zhang, New J. Chem. 43 (2019) 15596-15604.
- [81] J.E. Del Bene, I. Alkorta, J. Elguero, J. Phys. Chem. A 121 (2017) 8136–8146. [82] J.E. Del Bene, I. Alkorta, J. Elguero, ChemPhysChem. 18 (2017) 1597–1610.
- M. Liu, Q. Li, W. Li, J. Cheng, Struct. Chem. 28 (2017) 823-831.
- [84] M.D. Esrafili, F. Mohammadian-Sabet, E. Vessally, Mol. Phys. 114 (2016) 2115-
- [85] D. Pathak, S. Deuri, P. Phukan, J. Phys. Chem. A 120 (2016) 128-138. [86] I. Alkorta, F. Blanco, J. Elguero, J.A. Dobado, S.M. Ferrer, I. Vidal, J. Phys. Chem. A
- 113 (2009) 8387-8393. [87] J.E. Del Bene, I. Alkorta, J. Elguero, Chem. Phys. Lett. 685 (2017) 338-343.
- [88] H. Lv, H.-Y. Zhuo, Q.-Z. Li, X. Yang, W.-Z. Li, J.-B. Cheng, Mol. Phys. 112 (2014) 3024-3032.
- [89] C. Rest, A. Martin, V. Stepanenko, N.K. Allampally, D. Schmidt, G. Fernandez, Chem. Commun. 50 (2014) 13366-13369.
- [90] M.D. Esrafili, N. Mohammadirad, J. Mol. Model. 19 (2013) 2559-2566.
- [91] Q. Li, Y. Wang, Z. Liu, W. Li, J. Cheng, B. Gong, J. Sun, Chem. Phys. Lett. 469 (2009)48-51.
- [92] Q. Zhao, D. Feng, Y. Sun, J. Hao, Z. Cai, Int. J. Quantum Chem. 111 (2011) 3881-3887.
- [93] Z. Chi, T. Yan, Q. Li, S. Scheiner, J. Phys. Chem. A 123 (2019) 7288–7295.
- [94] V.D.P.N. Nziko, S. Scheiner, J. Phys. Chem. A 119 (2015) 5889–5897. [95] R. Taylor, 3.05 Progress in the Understanding of Traditional and
- Nontraditional Molecular Interactions, in: S. Chackalamannil, D. Rotella, S.E. Ward (Eds.), Comprehensive Medicinal Chemistry III, Elsevier, Oxford, 2017, pp. 67-100.
- [96] C. Trujillo, A. Rodriguez-Sanz, I. Rozas, Molecules 20 (2015) 9214.
- [97] A. Campo-Cacharrón, E.M. Cabaleiro-Lago, J.A. Carrazana-García, J. Rodríguez-Otero, J. Comput. Chem. 35 (2014) 1290–1301.
- Y. Zhao, Y. Cotelle, L. Liu, J. López-Andarias, A.-B. Bornhof, M. Akamatsu, N. Sakai, S. Matile, Acc. Chem. Res. 51 (2018) 2255-2263.